Transport of the graphene electrons through a magnetic superlattice

2008 J. Phys.: Condens. Matter 20 485210

(http://iopscience.iop.org/0953-8984/20/48/485210)

IOP PUBLISHING JOURNAL OF PHYSICS: CONDENSED MATTER

J. Phys.: Condens. Matter **20** (2008) 485210 (4pp) doi:10.1088/0953-8984/20/48/485210

Transport of the graphene electrons through a magnetic superlattice

Quan-Sheng Wu, Sheng-Nan Zhang and Shi-Jie Yang[1]

Department of Physics, Beijing Normal University, Beijing 100875, People's Republic of China

E-mail: yangshijie@tsinghua.org.cn

Received 1 July 2008, in final form 15 September 2008
Published 17 October 2008
Online at stacks.iop.org/JPhysCM/20/485210

Abstract

We studied the transport of graphene electrons through lateral magnetic barriers. The relativistic electrons experience resonant tunneling through two adjacent but opposite magnetic field regions. For a periodic structure fabricated with such magnetic barriers, the resonant tunneling peak further splits into several sharp spikes. The conductance also shows oscillation with the Fermi energy.

(Some figures in this article are in colour only in the electronic version)

1. Introduction

Recently, graphene has attracted tremendous interest from both theoretical and experimental physicists because of its gapless semiconductor property, which implies the possibility of extensive applications in nanoelectronics [1–7]. The linear dispersion relation of the graphene electrons was verified by direct observation of the unconventional quantum Hall effects at room temperature [8–10]. The Dirac-like quasi-electrons result in unusual consequences in the electronic transport properties, owing to its chiral characteristics. One of the peculiar phenomena is the complete transmission of Dirac fermions through a high enough electrostatic potential, or the so-called Klein paradox. However, this feature makes it a weakness for the graphene to be fabricated into a heterostructure since Dirac electrons cannot be confined by electrostatic potentials. Many attempts have been made to overcome this shortcoming [11–13].

Recently, several authors have proposed an alternative way of confining the graphene electrons by employing magnetic field barriers or magnetic quantum dots [14–16]. Virtually, mesoscopic transport through magnetic barriers has been extensively studied for Schrödinger electrons in conventional semiconductors [17–21]. In this work, we extend the analysis of [14] and discuss the properties of the graphene electrons tunneling through a lateral magnetic barrier as well as a magnetic superlattice. We study the extreme case that the magnetic field is uniform in a limited region. This means the asymptotic states are free waves so that the usual definition of transmission coefficient is well defined within the conventional transfer Hamiltonian formalism of the tunneling current. For a barrier which is composed of two magnetic field regions adjacent but opposite in direction, the incident electron experiences resonant tunneling according to its transport energy (the Fermi energy of the graphene). It is found that the transmission probability oscillates with the incident angles. When the electron transports through a magnetic superlattice (figure 1), then the resonant peaks further split into several sharp spikes. In general, for a n-period superlattice there are $(n-1)$ splitting spikes, similar to the case for the Schrödinger electrons [23]. The physical mechanism of the resonant transmission is discussed.

This paper is organized as follows. Section 2 describes the formalism. Section 3 presents the numerical results of the transport of the graphene electron by the transfer matrix method. We also discuss the implications of the resonant tunneling. Section 4 is a brief summary.

2. Formalism

We consider the ideal Dirac fermion in graphene with a lateral magnetic field perpendicular to the plane, $\mathbf{B} = B(x, y)\hat{\mathbf{e}}_z$. The static massless Dirac–Weyl equation for the spinor $\psi(x, y) = (\psi_+, \psi_-)^{\mathrm{T}}$ is

$$v_{\mathrm{F}}\boldsymbol{\sigma} \cdot \left[\mathbf{p} + \frac{e}{c}\mathbf{A}(x, y)\right]\psi(x, y) = \varepsilon\psi(x, y), \qquad (1)$$

[1] Author to whom any correspondence should be addressed.

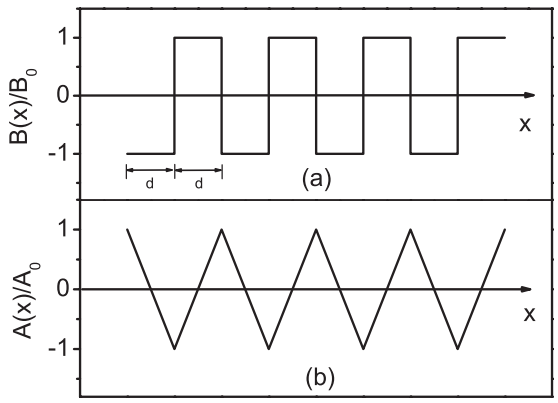

Figure 1. Schematic description of (a) the magnetic field and (b) the corresponding vector potential.

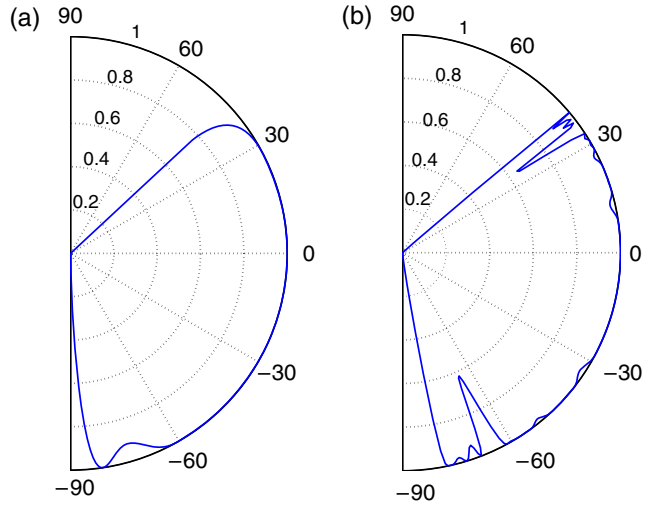

Figure 2. Polar graphs for the dependence of transmission coefficient T on incident angle θ. The radius of the semicircle represents the transmission coefficient T. (a) One period of the magnetic superlattice ($N = 1$) for $d = 2$ and $\varepsilon = 6.3$. (b) Four periods of the magnetic superlattice ($N = 4$) for $d = 2$ and $\varepsilon = 5$.

where $\mathbf{p} = -i(\partial_x, \partial_y)^{\mathrm{T}}$ is the momentum operator (setting $\hbar = 1$) and $\mathbf{A}(x, y)$ is the magnetic vector potential. $\boldsymbol{\sigma} = (\sigma_x, \sigma_y)$ are the 2×2 Pauli matrices. We set the Fermi velocity $v_{\mathrm{F}} = 1$.

We study a two-dimensional periodic magnetic field which is translation-invariant in the y direction and points alternatively up and down along the x direction, with a periodicity of $2d$ (see figure 1). The explicit expression is written as

$$B(x) = B_0 \sum_{n=0}^{2N-1} (-1)^n \theta(x - nd)\theta((n+1)d - x) \quad (2)$$

for $0 < x < 2Nd$ and $B(x) = 0$ otherwise. Here $\theta(x)$ is the Heaviside step function and N is the number of periods. By choosing the Landau gauge, the vector potential $\mathbf{A}(x, y) = (0, A(x), 0)$ has the sawtooth form in region II, i.e. $0 < x < 2Nd$:

$$A(x) = B_0 \sum_{n=0}^{2N-1} (-1)^n [x - (2n+1)d/2] \times \theta(x - nd)\theta[(n+1)d - x], \quad (3)$$

$A(x) = -B_0 d/2$ for region I, i.e. $x < 0$, and $A(x) = -B_0 d/2$ for region III, i.e. $x > 2Nd$. As the momentum in the y direction is conserved, equation (1) is reduced to two coupled equations:

$$[\partial_x \pm (k_y + A(x))]\psi_{\mp}(x) = \mathrm{i}\varepsilon\psi_{\pm}(x), \quad (4)$$

where k_y is the momentum in the y direction. Here all the quantities are set to dimensionless units by rescaling: the magnetic field $B(x) \to B_0 B(x)$, the vector potential $A(x) \to B_0 \ell_B A(x)$ with the magnetic length $\ell_B = \sqrt{c/eB_0}$, the wavevector $k \to k/\ell_B$, the electron energy $\varepsilon \to \varepsilon/\ell_B$, the coordinate $x \to \ell_B x$ and the width of a single magnetic barrier $d \to \ell_B d$. Consider an electron with wavevector $\mathbf{k} = (k_x, k_y)$ entering from the left region I at incident angle θ; one has $k_x = \varepsilon\cos\theta$, $k_y = \varepsilon\sin\theta + A(x)|_{x<0}$. The wavefunction in region I is written as

$$\psi_{\mathrm{I}}(x, y) = \begin{pmatrix} 1 \\ \mathrm{e}^{\mathrm{i}\theta} \end{pmatrix} \mathrm{e}^{\mathrm{i}k_x x + \mathrm{i}k_y y} + r \begin{pmatrix} 1 \\ -\mathrm{e}^{-\mathrm{i}\theta} \end{pmatrix} \mathrm{e}^{-\mathrm{i}k_x x + \mathrm{i}k_y y}. \quad (5)$$

The outgoing angle ϕ in region III is obtained by momentum conservation in the y direction:

$$\varepsilon\sin\phi + A(x)|_{x>2Nd} = \varepsilon\sin\theta + A(x)|_{x<0}. \quad (6)$$

Up to an overall normalization factor, the scattering state in region III is

$$\psi_{\mathrm{III}}(x, y) = t \begin{pmatrix} 1 \\ \mathrm{e}^{\mathrm{i}\phi} \end{pmatrix} \mathrm{e}^{\mathrm{i}k_x x + \mathrm{i}k_y y}. \quad (7)$$

The transmission coefficient $T = |t|^2$ is then calculated by the transfer matrix method [22].

According to the Landauer–Büttiker formulae, the ballistic conductance is calculated with the transmission coefficient as

$$G/G_0 = \int_{-\pi/2}^{\pi/2} T(\varepsilon_{\mathrm{F}}, \sqrt{2\varepsilon_{\mathrm{F}}}\sin\theta)\cos\theta\,\mathrm{d}\theta, \quad (8)$$

where θ is the incident angle and ε_{F} is the Fermi energy. $G_0 = 2e^2 m^* v_{\mathrm{F}} L_y/h^2$, where L_y is the width of the sample in the y direction, m^* is the effective mass of the graphene electron and v_{F} the Fermi velocity.

3. Numerical results

In the following, we have typically set $B_0 = 0.05$ T or $l_B = 115$ nm. We choose the length of one period of the magnetic superlattice as $2d = 2l_B$ and the corresponding transmission energy ranges from 0 to 39.8 meV. Figures 2(a) and (b), respectively, display the transmission coefficients of the electron transport through one period ($N = 1$) and four periods ($N = 4$) of the superlattice according to the incident angles. For the one-period case there is a resonant peak at $\theta \approx -80°$. In figure 2(b) the transmission probability begins to oscillate with the incident angles and the resonant

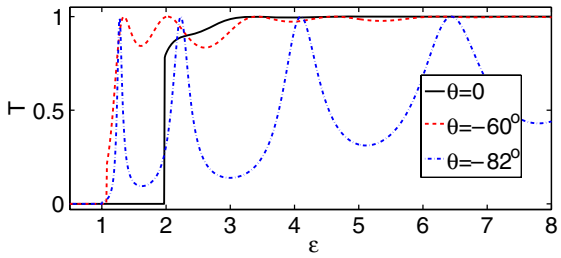

Figure 3. Energy dependence of the transmission T through a single magnetic barrier ($N = 1$) for incident angle $\theta = 0$ (solid curve), $\theta = -60°$ (dashed curve) and $\theta = -82°$ (dashed–dotted curve), respectively.

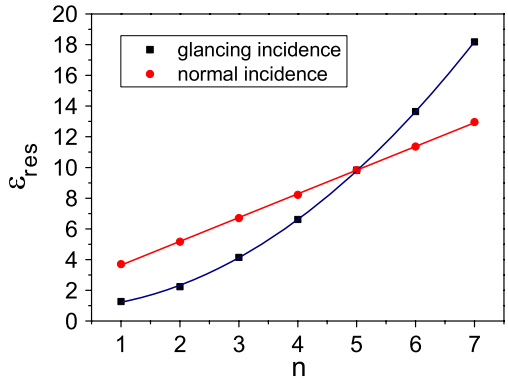

Figure 4. Resonant tunneling energy versus resonance number at normal (circles) and glancing (squares) incidence, which respectively reveal a linear and a quadratic relation.

peaks in the one-period case further split into three sub-peaks. In the mean time, the oscillation amplitudes become larger.

Figure 3 shows the energy dependence of the transmission probability for a single magnetic barrier ($N = 1$). It is not surprising that there are resonant tunnelings at some specific energies, as is observed in the case of Schrödinger electrons. In this figure we compare the differences between normal and glancing incidence. At glancing incidence, the resonant peaks become sharper. We observe that there are two distinct relations between the resonant number ($n = 1, 2, 3, \ldots$) and the resonant energy $\varepsilon_{\rm res}$. For normal incidence, the fitted curve shows $\varepsilon_{\rm res} \sim n$, whereas for glancing incidence, $\varepsilon_{\rm res} \sim n^2$ (see figure 4). The implications of these relations are accounted for as follows.

We change the magnetic gauge as $\mathbf{A}(x, y) = (A(y), 0, 0)$, with $A(y) = By$ for $0 < x < d$ and $A(y) = -By$ for $d < x < 2d$. The magnetic phase shifts $\Delta\phi_{\rm mag} = \int \mathbf{A}(\mathbf{r}) \cdot \mathrm{d}\mathbf{r} = \int A(y)\,\mathrm{d}x$ in the two opposite magnetic regions exactly offset. Hence the phase shift of the transporting electron wave is $\Delta\phi = 2k_x d$, which should satisfy the resonant condition, i.e. $\Delta\phi = 2n\pi$ (n is an integer). For the normal incidence ($k_y = 0$), $k_x = \varepsilon$ leads to $\varepsilon_{\rm res} = n\pi/d$. On the other hand, for the glancing incidence ($|k_x| \ll |k_y|$) of a momentum eigenstate in the y direction we have $\varepsilon_{\rm res} = \sqrt{k_x^2 + k_y^2} \approx k_y(1 + k_x^2/2k_y^2) \propto n^2$.

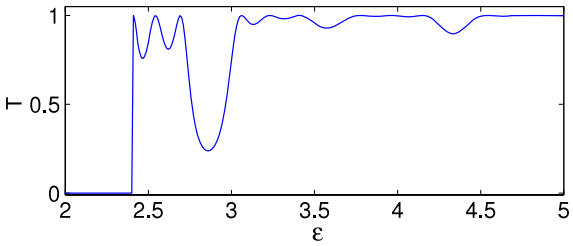

Figure 5. Energy dependence of transmission T through four periods of the magnetic superlattice ($N = 4$) at normal incidence.

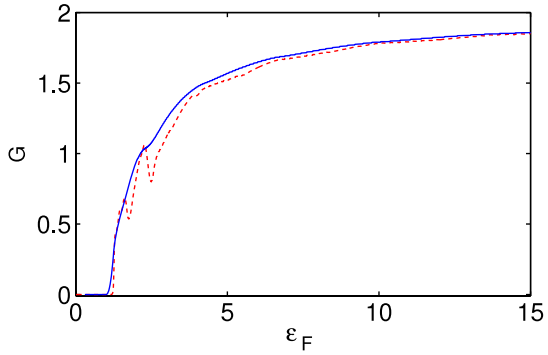

Figure 6. Energy dependence of the ballistic conductance through magnetic superlattices for $N = 1$ (solid curve) and $N = 4$ (dashed curve), respectively.

Figure 5 plots the transmission coefficient for four periods of the magnetic superlattice ($N = 4$). At normal incidence, the resonant peaks in the $N = 1$ case further split into a fine structure with $N - 1$ sub-peaks. This fine structure is analogous to the Fabry–Perot interference and was also found in the transport of the Schrödinger electrons [24].

Finally, we calculate the ballistic conductance of the graphene electrons by the Landauer–Büttiker formulae. Figure 6 shows the Fermi energy dependence of the conductance for one period (solid curve) and four periods (dashed curve) of the magnetic superlattice. It reveals the oscillating characteristics as in the Schrödinger electron cases. The more periods of the superlattice, the more prominent the oscillation becomes.

4. Summary

We have studied the transport of graphene electrons through a magnetic superlattice. The resonant tunneling reveals the same features as in the Schrödinger electron cases. The distinct relations of resonance between normal incidence and glancing incidence as well as their implications are discussed. We mention that our results are valid for such a sharply fluctuating magnetic field as well as for other periodic structures such as the sine function type. From the experimental aspect, nanodomains of magnetic superlattices had been constructed in (AlGa)As/GaAs heterostructures [25]. One expects that such magnetic complexes can also be built in current graphene samples.

Acknowledgment

This work is supported by the National Natural Science Foundation of China under grant nos 10574012 and 10874018.

References

[1] Semenoff G W 1984 *Phys. Rev. Lett.* **53** 2449
[2] Novoselov K S, Geim A K, Morozov S V, Jiang D, Zhang Y, Dubonos S V, Grigorieva I V and Firsov A A 2004 *Science* **306** 666
[3] Novoselov K S *et al* 2005 *Nature* **438** 197
[4] Geim A K and Novoselov K S 2007 *Nat. Mater.* **6** 183
[5] Berger C *et al* 2006 *Science* **312** 1191
[6] Xu Z, Zheng Q-S and Chen G 2007 *Appl. Phys. Lett.* **90** 223115
[7] Bunch J S *et al* 2007 *Science* **315** 490
[8] Gusynin V P and Sharapov S G 2005 *Phys. Rev. Lett.* **95** 146801
[9] Zhang Y, Tan Y W, Stormer H L and Kim P 2005 *Nature* **438** 201
[10] Novoselov K S, Jiang Z, Zhang Y, Morozov S V, Stormer H L, Zeitler U, Maan J C, Boebinger G S, Kim P and Geim A K 2007 *Science* **315** 1379
[11] Cheianov V V and Falko V I 2006 *Phys. Rev.* B **74** 041403
[12] Katsnelson M I, Novoselov K S and Geim A K 2006 *Nat. Phys.* **2** 620
[13] Silvestrov P G and Efetov K B 2007 *Phys. Rev. Lett.* **98** 016802
[14] De Martino A, Dell'Anna L and Egger R 2007 *Phys. Rev. Lett.* **98** 066802
[15] Peres N M R, Castro Neto A H and Guinea F 2006 *Phys. Rev.* B **73** 241403
[16] Matulis A and Peeters F M 2007 *Phys. Rev.* B **75** 125429
[17] Johnson M, Bennett B R, Yang M J, Miller M M and Shanabrook B V 1997 *Appl. Phys. Lett.* **71** 974
[18] Kubrack V *et al* 2000 *J. Appl. Phys.* **87** 5986
[19] Carmona H A, Geim A K, Nogaret A, Main P C, Foster T J, Henini M, Beaumont S P and Blamire M G 1995 *Phys. Rev. Lett.* **74** 3009
[20] Nogaret A, Bending S J and Henini M 2000 *Phys. Rev. Lett.* **84** 2231
[21] Guo Y, Gu B-L, Duan W-H and Zhang Y 1997 *Phys. Rev.* B **55** 9314
[22] You J Q *et al* 1995 *Phys. Rev.* B **52** 17243
[23] Tsu R and Esaki L 1974 *Appl. Phys. Lett.* **24** 593
[24] Pereyra P 1998 *Phys. Rev. Lett.* **80** 2677
[25] Duffield T *et al* 1986 *Phys. Rev. Lett.* **56** 2724